Quaternary Science Reviews 28 (2009) 977–990

Contents lists available at ScienceDirect

Quaternary Science Reviews

journal homepage: www.elsevier.com/locate/quascirev

# Natural hazards, extreme events, and mountain topography

Oliver Korup [a,*], John J. Clague [b]

[a] Swiss Federal Research Institutes WSL/SLF, CH–7260 Davos, Switzerland
[b] Centre for Natural Hazard Research, Simon Fraser University, Vancouver, B.C. V6B 1R8, Canada

ARTICLE INFO

*Article history:*
Received 25 February 2009
Accepted 27 February 2009

ABSTRACT

The hazard of any natural process can be expressed as a function of its magnitude and the annual probability of its occurrence in a particular region. Here we expand on the hypothesis that natural hazards have size–frequency relationships that in parts resemble inverse power laws. We illustrate that these trends apply to extremely large events, such as mega-landslides, huge volcanic debris avalanches, and outburst flows from failures of natural dams. We review quantitative evidence that supports the important contribution of extreme events to landscape development in mountains throughout the world, and propose that their common underreporting in the Quaternary record may lead to substantial underestimates of mean process rates. We find that magnitude–frequency relationships provide a link between Quaternary science and natural hazard research, with a degree of synergism and societal importance that neither discipline alone can deliver. Quaternary geomorphology, stratigraphy, and geochronology allow the reconstruction of times, magnitudes, and frequencies of extreme events, whereas natural hazard research raises public awareness of the importance of reconstructing events that have not happened historically, but have the potential to cause extreme destruction and loss of life in the future.



## 1. Introduction

Over the past several thousand years, extreme geological events have killed tens of millions of people and severely damaged human infrastructure (Fig. 1). Some geological events may have even shaped the course of early civilisations, including, for example, the Minoans in the Mediterranean, the Vikings in Greenland, and the Mayans in Central America (e.g. Sparks et al., 2005; Cashman and Giordano, 2008; Nur and Burgess, 2008).

Potentially harmful geological, climatic, and hydrologic processes are subject of the rapidly growing field of natural hazards research. The term "hazard" expresses the likelihood that a potentially damaging event will occur within a particular region during a specified period of time (e.g. Cruden and Varnes, 1996). Natural hazards can be quantified statistically from documented time series using historical data, but the time series are typically short and may not capture the full range of process magnitudes. For example, the 2004 Indian Ocean tsunami, which killed more than 225,000 people in 11 countries, is regarded as an extreme event based on the brief historic record, but geological data show that tsunami of the same size are common in the Indian Ocean on timescales of hundreds to thousands of years (Jankaew et al., 2008; Monecke et al., 2008). In this respect, the geological record provides a unique context for evaluating hazards posed by extreme events. The innate interdisciplinarity of Quaternary research offers many opportunities for identifying traces left by extreme events in the geological record.

Here, we amplify on the papers in this Special Issue by arguing that Quaternary science and natural hazards research, two cross-cutting but traditionally unrelated fields, have much in common, as well as considerable potential for synergism – in combination they can produce results of societal importance that neither discipline on its own can deliver. On one hand, Quaternary science provides the necessary tools for reconstructing ages and frequencies of prehistoric extreme events that are recorded in landforms and sediments. Geomorphology and stratigraphy provide additional information on the magnitude of past events and the underlying climatic and environmental conditions that prevailed at the time of the events. For its part, natural hazard research provides a context for raising awareness of the importance of reconstructing events that have not happened in the historic period, yet have the potential to cause much destruction and loss of life in the future (Messerli et al., 2000).

We focus here on mountainous terrain, which is the product of an interplay among tectonic, climatic, and erosional processes. Pronounced tectonic and climatic forcing, manifest in high rock

* Corresponding author. Tel.: +41 81 417 0250; fax: +41 81 417 0110.
*E-mail address:* korup@slf.ch (O. Korup).

0277-3791/$ – see front matter © 2009 Elsevier Ltd. All rights reserved.
doi:10.1016/j.quascirev.2009.02.021

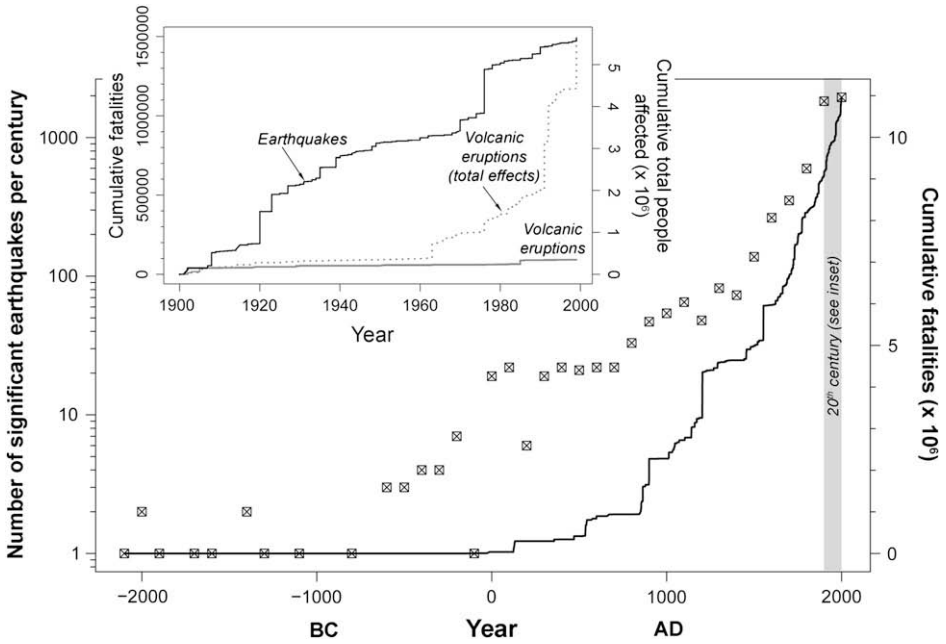


**Fig. 1.** Number of significant earthquakes per century for the past 4000 years (crossed squares), and the cumulative minimum number of associated fatalities (black line; data obtained from the National Geophysics Data Center, http://www.ngdc.noaa.gov). Nearly 6000 earthquakes during this period have claimed at least 11 million lives. All events recorded here caused at least US$1 million damage, claimed more than 10 lives, had a magnitude > 7.5 or Mercalli Intensity > X, or triggered a tsunami. Inset shows cumulative fatalities caused by 2522 earthquakes during the 20th century compared to those caused by 491 volcanic eruptions (Witham, 2005); the total number of people affected by these eruptions is also shown.

uplift rates, recurring large earthquakes, orographically enhanced precipitation, and high rates of mass wasting, erosion, and sediment transport create landscapes of high topographic relief and steep slopes. Extreme events in such settings leave characteristic proxy records that can be exploited through Quaternary research. We highlight magnitude–frequency relationships of selected natural hazards and argue that extreme events play a pivotal role in erosion, sediment flux, and landscape development. At the same time, mountain belts have seen substantial increases in human presence, and thus elevated potential of adverse impact by such extreme events.

It is not our goal to provide a comprehensive review of previous work on natural hazards and extreme events in mountain belts. This body of literature is large and growing, and cannot be captured in an introduction to the papers assembled in this issue. Rather we provide examples of more recent research that showcase the interface between Quaternary science and natural hazards and that demonstrate the synergy between the two.

## 2. Magnitude, frequency, and hazard

Research over the past decades has increasingly demonstrated that many natural and potentially hazardous geological processes are characterised by nonlinear relationships between size and frequency (Fig. 2). The well-known Gutenberg–Richter relation is a prime example and has long been used to characterise earthquake frequency as a function of magnitude. Similarly, inverse power laws have been proposed to describe at least parts of the frequency–magnitude distributions of landslides, wildfires, windstorms, and other natural processes (Turcotte et al., 2002). Although testing of this power-law hypothesis has rarely been rigorous (Clauset et al., 2007), one of its important benefits is that it helps quantify hazards and the geomorphic efficacy of the processes involved.

A reliable estimation of the hazard of a given process requires a reasonably complete inventory of well-dated events of known size and a sound statistical model. Most quantitative hazard assessments, however, rely on time series of short duration that generally do not include rare, extreme events.

Several extreme-value distributions have been proposed for estimating the recurrence of large events. For example, the

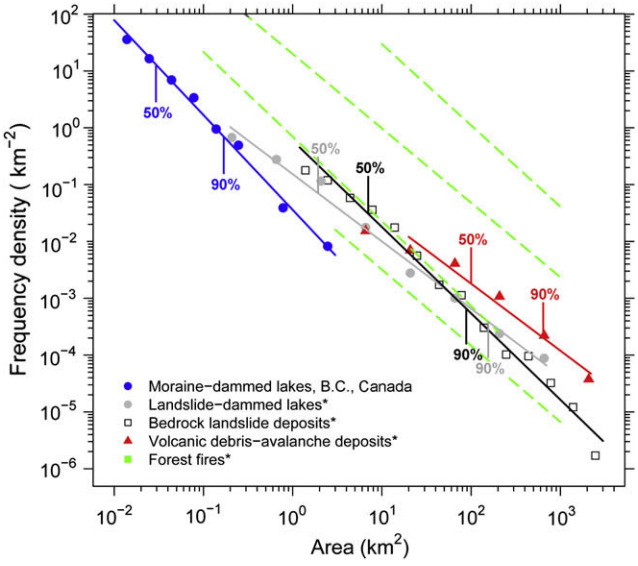


**Fig. 2.** Frequency–area distributions for hazardous geological processes in mountainous terrain (* indicates worldwide data). The size distribution of Neoglacial moraine-dammed lakes in British Columbia (McKillop and Clague, 2007), landslide-dammed lakes, bedrock landslides and volcanic debris avalanches (Korup et al., 2007), and forest fire areas (Turcotte et al., 2002) can be modelled by an inverse power law. Straight lines are best-fit geometric mean regressions on log-binned density data. Vertical lines are 50th and 90th percentiles of cumulative area.

Log-Gumbel distribution (Whitehouse and Griffiths, 1983) has a density function:

$$p(V;V_0,u,\alpha) = \exp\left[-\exp\left(-\frac{\ln(V-V_0)-u}{\alpha}\right)\right], \quad (1)$$

where $V$ is event volume, $V_0$ is an arbitrarily set threshold volume, $u$ is a location parameter, and $\alpha$ is a scale parameter. This distribution assumes a Poisson (stochastic) arrival process and allows the volume of an event exceeding $V_0$ to be expressed as a function of its return period $T$:

$$V - V_0 = e^u\left[\left(\ln\frac{\lambda T}{\lambda T-1}\right)^{-\alpha}\right], \quad (2)$$

where $\lambda$ is the average rate at which events arrive. Hazard $H$ is expressed as the probability of occurrence of at least one event of return period $T$ in $z$ years:

$$H = 1-\left(1-\frac{1}{T}\right)^z \quad (3)$$

Alternative statistical models make no assumptions about the arrival process of extreme events. Malamud et al. (2004) investigated the relationship between landslide frequency and magnitude using three historical landslide inventories, each of which consists of several thousand, mainly small ($<1$ km$^2$) slope failures triggered by earthquake shaking, precipitation, and snowmelt. They found that an inverse gamma distribution provided the best fit to the probability density functions $p$ derived from all three inventories, regardless of geographic location, geology, topography, climate, or triggering mechanisms:

$$p(A_L;\rho,a,s) = \frac{1}{a\Gamma(\rho)}\left[-\frac{a}{A_L-s}\right]^{\rho+1}\exp\left[-\frac{a}{A_L-s}\right], \quad (4)$$

where $\Gamma(\rho)$ is the gamma function, $A_L$ is landslide planform area (km$^2$), $\rho = 1.40$ is the scaling exponent of the power-law tail in cumulative form, and $a$ and $s$ are scaling parameters with values $a = 1.28\times10^{-3}$ km$^2$ and $s = -1.32\times10^{-4}$ km$^2$. This model implies that the frequency of the largest landslides follows an inverse power-law relationship:

$$p(A_L) = a_A A_L^{-\alpha_A}, \quad (5)$$

where $a_A$ is a dimensional coefficient and $\alpha_A$ ($\approx\rho+1$) is the landslide-area scaling exponent. Most landslide inventories, however, are based on air photo interpretation and mapping, and thus are limited to small, frequent events ($A_L < 10^6$ m$^2$). Thus it remains unknown whether the model's power-law tail is indeed applicable for large events ($A_L > 10^6$ m$^2$). Below we present evidence that this is the case, not only for landslides but also a range of other natural processes.

## 3. Large earthquakes

### 3.1. Reconstructing large prehistoric events

Earthquakes are among the most destructive geological processes on Earth, having caused an estimated minimum of 11 million fatalities in the past 4000 years (Fig. 1). Recorded destructive earthquakes have increased by three orders of magnitude over this period, due not to any significant change in seismicity, but rather to the increasingly detailed documentation of younger events and to the increase in human population.

Reconstruction of pre-instrumental earthquakes is the subject of palaeoseismology (Bull, 2008). This discipline employs several methods to reconstruct and date seismic events (Chapron et al., 2006). One of the most important methods is fault trenching complemented by $^{14}$C dating of offset layers or post-rupture sag ponds. Much of our knowledge of long-term slip rates on active faults in California has been obtained using this method (e.g., McGill and Sieh, 1993; Yeats, 2001; Jing et al., 2006; Meltzner et al., 2006), and the technique has been widely used in other parts of the world to better understand frequency–magnitude relations of crustal earthquakes (e.g., Klinger et al., 2003; Lavé et al., 2005). Similarly, $^{10}$Be surface exposure dating of landforms such as fluvial terraces, fans, or moraines offset by active faults helps constrain slip rates and associated earthquake activity (Brown et al., 2002). However, inferred rates may differ by up to a factor of five depending on whether ages of the foot or the hanging wall are used (Cowgill, 2007).

Great earthquakes at subduction zones have been identified from the crustal uplift and subsidence they produce (Clague, 1997; Natwidjaja et al., 2007; Shennan et al., 2009). In the Pacific Northwest of the United States and southwest British Columbia, for example, coseismic subsidence during great earthquakes at the Cascadia subduction zone, which borders the Cascade Range to the east, is archived in tidal wetlands. The characteristic earthquake stratigraphy comprises a sequence of marsh peat layers, each abruptly overlain by tidal mud (Fig. 3; Atwater and Hemphill-Haley, 1997; Clague, 1997). Tsunami that accompanied the subduction earthquakes are recorded by landward-thinning and fining beds of sand directly overlying the subsided marsh peats (Clague and Bobrowsky, 1994; Clague et al., 2000). Tsunami sand layers also occur in the stratigraphies of low-lying coastal lakes (Hutchinson et al., 2000; Kelsey et al., 2005).

Dendrochronology offers precise dating of earthquakes by establishing the time of death of trees that subside into the tidal zone (Jacoby et al., 1997; Yamaguchi et al., 1997) or the germination dates of trees that become established on surfaces elevated above sea level during earthquakes. In New Zealand, Wells et al. (1999, 2001) dated tree cohorts on fluvial fill terraces formed by sediment pulses following earthquakes on the Alpine Fault on the west side of the Southern Alps; additional supporting evidence is found in the large outwash plains of the foreland (Fig. 4). Independent investigations of tree ages on subparallel coastal dune ridges corroborate the inferred times of ruptures on the Alpine Fault and a model of pulsed post-seismic sediment delivery by steep mountain rivers to the nearby coast (Wells and Goff, 2006).

Lichenometric studies of rock-fall debris have provided estimates of the ages of large earthquakes in New Zealand and the western United States, the assumption being that the rock falls were seismically triggered and that lichens became established on the fresh debris soon after it was emplaced (Bull, 2008). Large earthquakes also produce subaqueous landslides that can be dated to establish event ages (Karlin et al., 2004; Strasser et al., 2006). However, caution is required when interpreting the triggers of such mass movements, as they may be similarly produced by aseismic loading and collapse within a normal cycle of lake-delta growth (Girardclos et al., 2007). To circumvent such potential shortcomings, Schwab et al. (2009) conducted a multi-proxy study of lake sediments deposited within the North Anatolian Fault Zone and tentatively correlate several "event layers" with large historic earthquakes.

A comparably novel subdiscipline of palaeoseismological research is earthquake archaeology (Nur and Burgess, 2008). It uses geological and archaeological methods to date large earthquakes and infer their consequences in seismically active regions such as the Mediterranean.

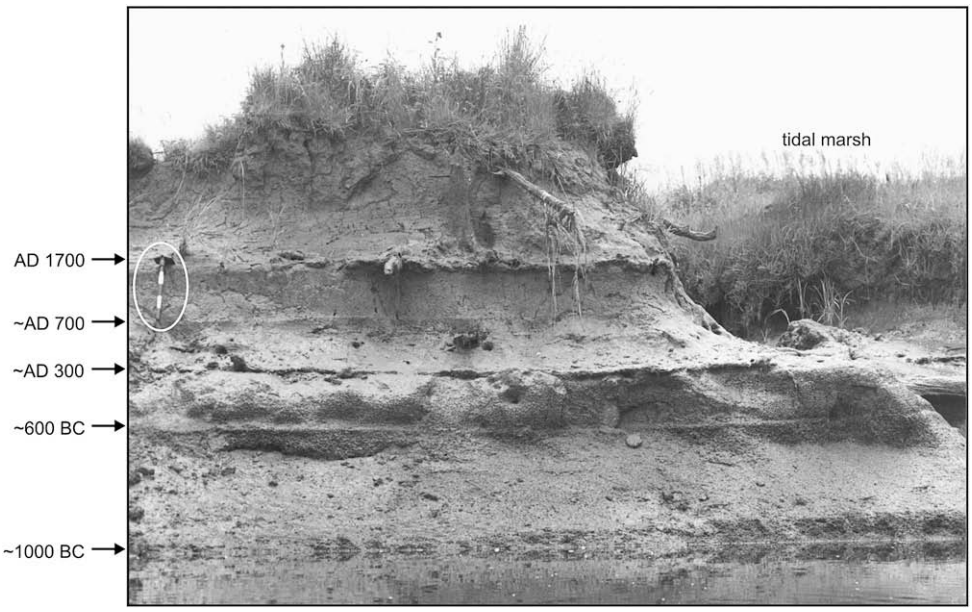


**Fig. 3.** Sequence of upper intertidal marsh peats (arrows) abruptly overlain by tidal muds exposed in the bank of the Niawiakum River, southwest Washington state, United States. Each peat subsided 1–2 m during a great earthquake at the Cascadia subduction zone. The approximate ages of the earthquakes are indicated at the left (Clague et al., 2006, based on information in Atwater and Hemphill-Haley, 1997).

### 3.2. Earthquakes as triggers of sediment pulses

Large earthquakes in mountainous terrain may trigger hundreds to ten thousands of landslides (Keefer, 1999). The landslides deliver large amounts of sediment to river channels, particularly in areas of orographically enhanced precipitation. They also perturb the fluvial system by forming natural dams, increasing sediment loads, aggrading valley floors, and destabilising channels. These effects are propagated as sediment waves until subsequent incision restores pre-earthquake flow regimes (Owen et al., 1996, 2008; Dadson et al., 2004).

Keefer (1999) argued on the basis of an empirical relation that coseismic sediment production is related to earthquake magnitude. Data from some recent events, however, suggest that this relation is not universally valid – some large earthquakes have produced far less sediment than would be predicted (e.g. Jibson et al., 2006). These data raise important question about the geomorphic efficacy of earthquakes in terms of the roles played by topography, rock type, hydrology, and other factors. In addition, the timescale at which earthquake-produced sediment is delivered to, and routed through, the drainage network is crucial in controlling erosion (Lin et al., 2008). Sediment generation by earthquakes may significantly affect long-term landscape evolution if the average return period of major sediment pulses is short, overwhelming the effect of background erosion. The delivery of earthquake-produced sediment to the drainage system, however, differs regionally and temporally (Owen et al., 1996, 2008; Dadson et al., 2004). In humid mountains with frequent high-intensity rainstorms, high runoff facilitates rapid transfer of landslide debris to streams; suspended sediment yields are typically several times higher than background rates (Dadson et al., 2004). In contrast, in arid orogens, sediment transfers may be delayed and more protracted (Keefer and Moseley, 2004).

Goff and McFadgen (2002) summarised a variety of types of geomorphic response to prehistoric large earthquakes in New Zealand and argued that recurrent large earthquakes are more important than climate and humans in effecting environmental change (Fig. 5). Detecting such process causality is crucial for convincingly linking independent proxy records and reconstructing the magnitude and effects of prehistoric earthquakes (Becker et al., 2005).

## 4. Volcanic eruptions

Volcanic eruptions are among the most effective agents of geomorphic change on Earth in terms of geologically instantaneous debris production (Fig. 6). Isotopic fingerprinting, tephrochronology, and $^{40}Ar/^{39}Ar$ dating are indispensable tools for estimating the frequency of volcanic eruptions during the Quaternary and thus their impact on the landscape (Allen et al., 2008).

As in the case of earthquakes, the magnitude of volcanic eruptions tends to follow an inverse power law (e.g. Pyle, 2000),


**Fig. 4.** Buried and exhumed forest soil in the lowland west of the Southern Alps, New Zealand. Numerous tree trunks in original growth position indicate sudden burial by several metres of river sediments. The forest was buried ~1400 years ago, possibly shortly after a large prehistoric earthquake on the Alpine Fault. Aseismic cycles of aggradation and degradation, however, produce comparable field evidence (Korup, 2004).

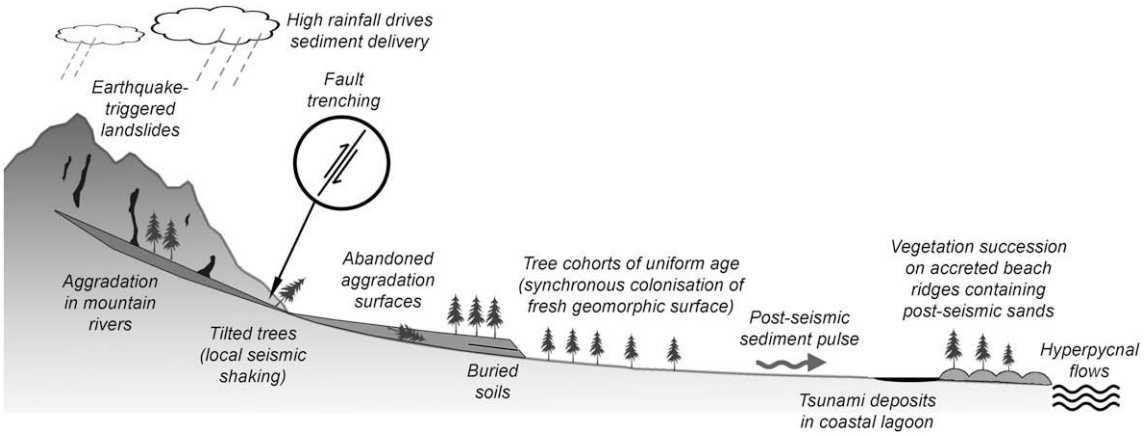


**Fig. 5.** Geomorphic legacy of earthquake-induced landslides and subsequent fluvial sediment pulses from the Southern Alps, New Zealand (not to scale; based on the "seismic staircase" model of Goff and McFadgen, 2002). Reconstructions of prehistoric earthquakes are most reliable when supported by several lines of evidence. Explosive volcanic eruptions may produce similar landform-sediment assemblages. The preservation potential of these different archives depends on the magnitude and frequency of the events that produce the sediment.

although alternative models are also used (Connor et al., 2003). Small eruptions with volumes of $10^4$–$10^5$ m$^3$ are common (Witham, 2005), but volumes of historical eruptions range through ten orders of magnitude (Thorardson and Larsen, 2007). At the far end of the spectrum are rare eruptions of super-volcanoes that release $>10^{10}$ m$^3$ of tephra and leave calderas tens of kilometres in diameter (Sparks et al., 2005). By comparison, the cataclysmic Mount St. Helens eruption in May 1980 released only $10^9$ m$^3$ of tephra, a mere 1% of the volume of the eruption from the Yellowstone volcanic centre 2.1 Ma ago.

The numerous back-arc volcanoes along subduction zones bordering the Pacific Ocean are set within mountainous landscapes where eruptions are accompanied by lateral blasts, flank collapses, large debris avalanches, and lahars. Pyroclastic flows may produce thick blankets of ignimbrite that fossilise or reshape large ($>10^3$ km$^2$) tracts of landscapes by filling topographic depressions, disrupting drainage networks, and causing widespread knickpoint formation and retreat (Fig. 7; Manville et al., 2005). Large eruptions deliver huge amounts of debris to rivers and may elevate short-term sediment yields to as high as $10^6$ m$^3$ km$^{-2}$ a$^{-1}$. High sediment yields are facilitated by a lack of vegetation, reduced infiltration, and enhanced runoff (Major et al., 2000; Gran and Montgomery, 2005).

Some of the largest landslides on Earth, with volumes $>10^9$ m$^3$, occur on the flanks of volcanic edifices (Fig. 2; Waythomas et al., 2009). Ponomareva et al. (2006) summarised the late Quaternary history of volcanic debris avalanches and flank collapses in southeast Kamchatka. Seventeen Holocene landslides in that area have produced nearly $3.5 \times 10^{10}$ m$^3$ of sediment, equal to a mean erosion rate of 0.04 mm a$^{-1}$ for the total area of the volcanic edifices.

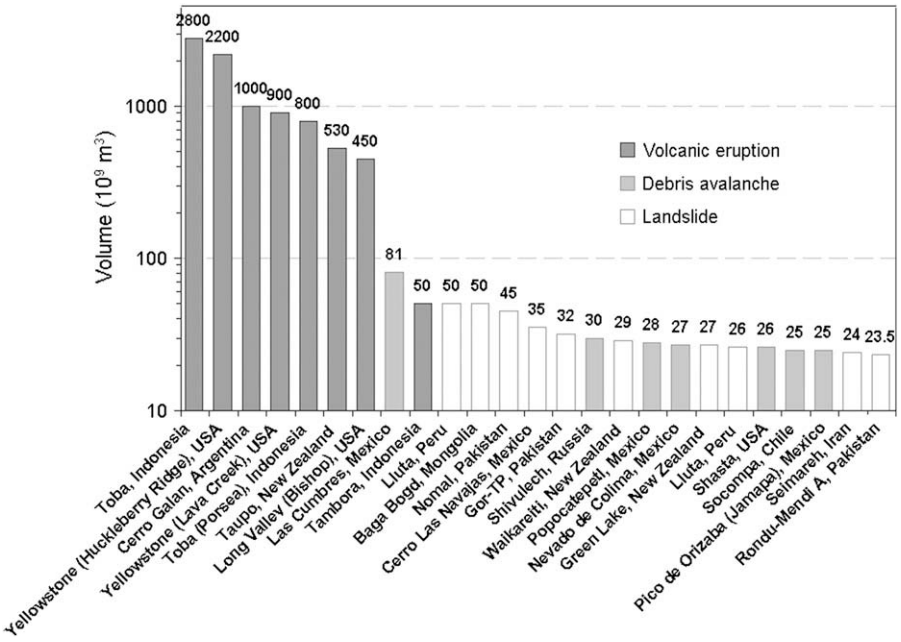


**Fig. 6.** The 25 largest debris-generating events in the Quaternary. The events are mainly volcanic eruptions, volcanic debris avalanches, and catastrophic bedrock landslides. Eruptive volumes are expressed in rock density equivalents. Submarine landslides are known to mobilise volumes in excess of $10^{12}$ m$^3$, but are not included here. Data mainly from Mason et al. (2004) and Korup et al. (2007).

**Fig. 7.** Large earthquakes and volcanic eruptions commonly cause significant geomorphic response in mountain rivers. Knickpoint formation and headward migration, and rapid incision attest to adjustments rivers of to newly formed base levels such as here at Dettifoss, Iceland.

In comparison, only four debris avalanches in the 20th century have moved material, equivalent to a mean erosion rate of 0.31 mm $a^{-1}$. Assuming that debris-avalanche activity has not increased substantially during the 20th century, this order-of-magnitude discrepancy points at potential under-sampling of older events. Nevertheless, the erosional efficacy of these few extreme events is enormous.

Super-volcanoes are located in areas of thin crust above shallow pools of highly evolved, siliceous magmas. In these areas, mantle plumes create high heat flows that elevate crustal temperatures to near 1000 °C at depths less than 10 km. Most super-volcanoes are located in the western United States (Yellowstone, California, New Mexico), the North Island of New Zealand, and Indonesia. No super-eruptions have occurred in historic time, but many are known from the geologic record (Fig. 6), including three huge eruptions from the Yellowstone volcanic centre (640 ka, 1.3 Ma, and 2 Ma), one that formed Lake Taupo in New Zealand (26 ka), and another that formed Lake Toba in Sumatra (74 ka) (Mason et al., 2004; Sparks et al., 2005). A similar eruption today would be catastrophic due to ash fall thousands of kilometres from the volcano (Sparks et al., 2005). Huge volumes of sulphur dioxide and other aerosols released into the atmosphere would also contribute to cooling climate. The ~74 ka Toba eruption, the largest known in the Quaternary, was about 2000 times larger than the 1980 Mount St. Helens eruption. It triggered massive environmental change and may have reduced the entire human population to <10,000 survivors (Ambrose, 1998), creating "population bottlenecks" in the several human species that existed at the time and accelerating differentiation of the isolated human populations. Ambrose (1998) hypothesized that the event eventually led to the extinction of all human species except for the two branches that became Neanderthals (*Homo neanderthalensis*) and modern humans (*Homo sapiens*). Although Ambrose's hypothesis has been contested (Oppenheimer, 2002), an eruption the size of the Toba event clearly would have global consequences.

## 5. Catastrophic rock-slope failures

### 5.1. Large infrequent events: hazard and erosion

Large (>$10^6$ $m^3$) landslides play a significant role in limiting topographic relief and modulating sediment flux in mountainous terrain (Korup, 2006; Hewitt et al., 2008). Hancox and Perrin (2009) describe the Green Lake landslide, which occurred at the close of the last glaciation in the Fiordland mountains of New Zealand. Its volume of $2.7 \times 10^{10}$ $m^3$ places it among the largest ten terrestrial, non-volcanic landslides on Earth (Korup et al., 2007) and among the 25 events that have mobilised the largest volumes of debris in the Quaternary (Fig. 6).

Steep slopes and high local relief are conducive to many such giant slope failures, consequently they are common in the Himalayas (Korup et al., 2007). Yet, known landslides in the Himalayas affect <1% of the orogen's total area, as opposed to ~10% in the Alps (Abele, 1974), which have much less relief and are tectonically less active. This difference points at significant under-sampling of such events, and their role is probably much greater than currently believed (Hewitt et al., 2008).

Whitehouse and Griffiths (1983) pioneered the use of the Log-Gumbel relation (Equation (1)) in quantifying the hazard from such large landslides. They estimated the annual probability of catastrophic rock avalanches in the central Southern Alps of New Zealand. Fourteen of their sample of 42 events are $>2 \times 10^7$ $m^3$ and were assumed to be the complete population of this size over the past 10,000 years. According to their model, a rock avalanche with a volume of $5 \times 10^7$ $m^3$ has an estimated return period of 3065 a in the Southern Alps; in contrast, one with a volume of $3.2 \times 10^8$ $m^3$ occurs every 10,000 years (a and b, respectively, in Fig. 8). Based on the record of several historic rock avalanches in the same area, McSaveney (2002) surmised that the data of Whitehouse and Griffiths (1983) likely yielded underestimates of the true frequency of rock avalanches in the Southern Alps, thus highlighting the strong dependence of the method on the documented record of events.

Inventories of large catastrophic landslides with known ages in the Alps and China can be similarly fitted with the Log-Gumbel distribution. In the Alps, the recurrence times of 31 dated rock avalanches $>2 \times 10^7$ $m^3$ during the past 10,000 years are exponentially distributed ($\lambda = 1/338$ $a^{-1}$, Equation (2)). Their average frequency is nearly twice that of rock avalanches in the New Zealand Southern Alps, but when normalised by the size of the study area, it reduces to ~2%. However, nearly half of the 68 known rock avalanches $>2 \times 10^7$ $m^3$ in the European Alps are undated, thus the time series is incomplete (Prager et al., 2008). If, for example, a total of 100 rock avalanches of $V > V_0$ occurred during the past 10,000 years, $T \sim 100$ a for an event $2 \times 10^7$ $m^3$ in size, and $T \sim 1.8 \times 10^4$ a for one of $1.3 \times 10^{10}$ $m^3$, which is the size of the Flims rock slide, the largest landslide in the European Alps. The return period of this largest event ($\sim 1.8 \times 10^4$ a) essentially remains the same whatever the number of unrecorded smaller events.

Similarly, Equation (5) and related distributions have been applied to a number of landslide inventories throughout the world, but it remains uncertain whether the proposed power-law tail is valid for large catastrophic events (Dussauge et al., 2003). Landslide volumes $V_L$ of 68 Holocene catastrophic landslides in the European Alps (Abele, 1974; Korup et al., 2007; Prager et al., 2008) have a scaling exponent $\alpha_V = 1.32 \pm 0.06$ ($\pm 1\sigma$; Fig. 9). Expanding the sample to 110 Lateglacial and Holocene (i.e. post-16 ka) landslides in the Alps produces the same scaling exponent, $\alpha_V = 1.32 \pm 0.08$, suggesting that the relationship yields a reliable first-order estimate of large landslide recurrence. The Holocene rock avalanches documented by Whitehouse and Griffiths (1983) yield a similar scaling exponent, whereas the fit to large 20th century landslides in China is steeper (Fig. 9). Importantly, we find that $\alpha_V < 2$ in all cases, which implies that fewer and larger landslides mobilise substantial fractions of the total debris volume, thus dominating the volumetric production rate of sediment.

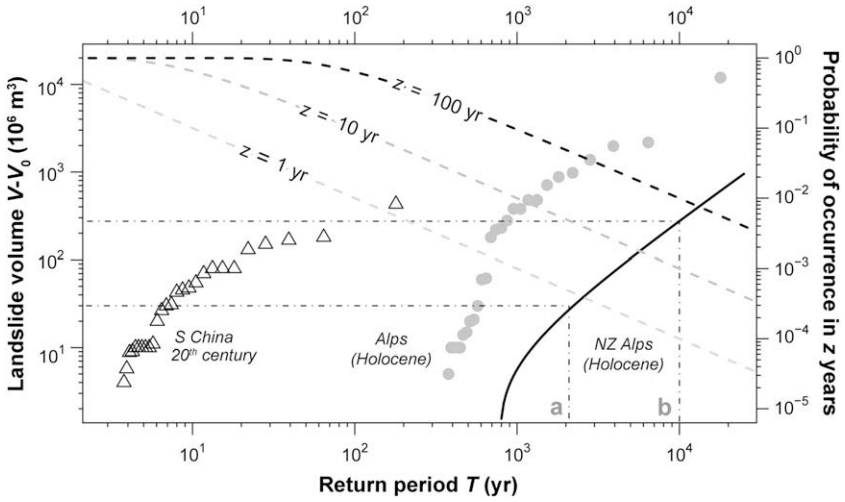


**Fig. 8.** Average return periods for three sets of landslides with volumes $(V - V_o) > 2 \times 10^7$ m$^3$ (Equation (2)): 35 events in south-central China in the 20th century (Wen et al., 2004); 31 Holocene bedrock failures, European Alps (Abele, 1974; Korup et al., 2007; Prager et al., 2008); and 14 Holocene rock avalanches in the central Southern Alps, New Zealand (curve based on Equation (1); Whitehouse and Griffiths, 1983). The large differences in return periods for a given landslide volume are partly due to order-of-magnitude differences in the sizes of the study areas, i.e. $10^6$, $10^5$, and $10^4$ km$^2$, respectively. The right *y*-axis indicates the probability of occurrence of an event with a known return period *z* of 1, 10, and 100 years (dashed lines).

### 5.2. *Proxies of palaeoclimate or palaeoearthquakes?*

Large landslides are mainly triggered during large earthquakes (Keefer, 1999; Dunning et al., 2007) and high-intensity rainstorms. They are, therefore, potential proxies of past seismic and climate events (Crozier et al., 1995; Mitchell et al., 2007). Yet landslide deposits have been underexploited in this regard, mainly because the number of well-dated landslides in any area is small (Bookhagen et al., 2005; Capra, 2006; Strom and Korup, 2006; Dortch et al., in this issue; Hewitt, 2009). In this regard, younger landslide deposits may allow more reliable reconstructions, mainly because small and moderate deposits have relatively short residence times in the landscape (Fig. 10). This important finding highlights the potential for censoring of smaller events from the geological record, either through erosion or deposition by subsequent processes. A consequence of this censoring is that more reliable statements on possible relations between climate change and landslide occurrence can be made for the recent geological past. For example, Holm et al. (2004) showed that glacier downwasting and retreat following the Little Ice Age caused increased slope instability in the upper Lillooet River valley in British Columbia – most of the landslides detached near or beneath conspicuous Little Ice Age glacier trimlines.

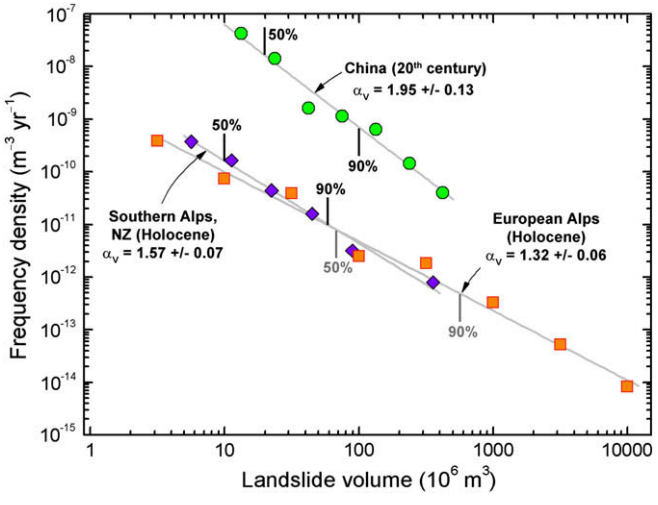


**Fig. 9.** Frequency density as a function of volume for 70 large landslides in China in the 20th century (Wen et al., 2004), 44 Holocene rock avalanches in the Southern Alps of New Zealand (Whitehouse and Griffiths 1983), and 68 Holocene landslides in the European Alps (Abele, 1974; Korup et al., 2007; Prager et al., 2008). Exponents $(-\alpha_V)$ of geometric mean regression equations have values <2, showing that larger landslides dominate the volumetric production of sediment. Vertical bars are 50th and 90th percentiles of cumulative volumes. Data are from the same inventories as those used to produce Fig. 8, but also include smaller landslides.

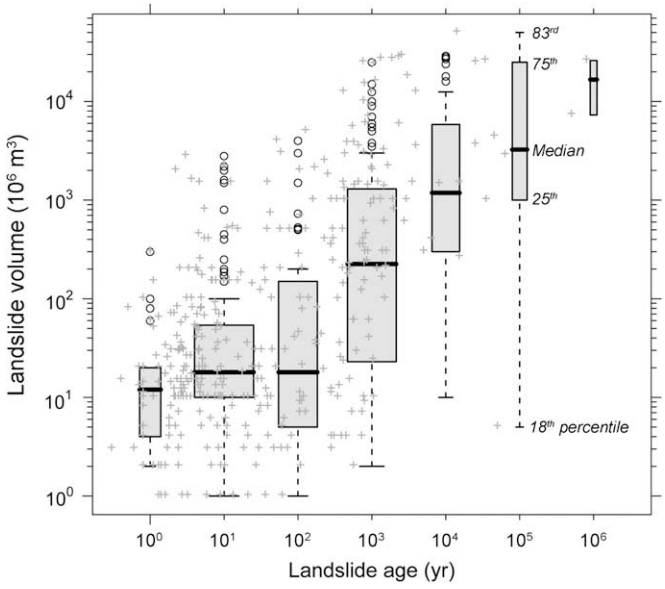


**Fig. 10.** Event size and preservation of geomorphic evidence in the landscape. Box and whisker plot shows the age–size distribution of 393 bedrock landslides of volumes $>10^6$ m$^3$ throughout the world (grey crosses are raw data). Box width is proportional to the square root of sample number log-binned by time interval. The distinct lack of smaller deposits of greater age indicates that deposits of larger landslides remain in the landscape much longer than those of smaller events, despite the broad range of climatic and tectonic settings, and erosion rates that the data encompass.

Detection and study of deposits of large bedrock landslides may have significant consequences for palaeoclimatic reconstructions. Debris piles formed by catastrophic rock avalanches have been misinterpreted as glacial moraines in some mountain ranges (Fig. 11). Many of these "moraines" are central to published glacial chronologies, and erroneous climatic inferences have been advanced to explain their origin (Hewitt, 1999). Further, catastrophic landslides onto glaciers may trigger surges that have no climatic significance (Hewitt, 1988). Deline (2009) reports several such rock avalanches onto glaciers on the Mont Blanc massif in the European Alps since the Little Ice Age. His study highlights the importance of these events in eroding steep bedrock slopes and delivering large amounts of sediment to valley glaciers, potentially influencing their dynamics (see also Hambrey et al., 2008). Tovar et al. (2008) and Shulmeister et al. (2009) further discuss the possibility that large bedrock landslides onto glaciers in the Southern Alps of New Zealand can trigger advances that produce lateral and end moraines without any causal link to climate (Fig. 12). They build on earlier work by Larsen et al. (2005), who argued that the debris forming large moraines at the west front of the Southern Alps of New Zealand has an earthquake origin.

### 5.3. Landslide tsunami

Large catastrophic rock-slope failures can also trigger destructive tsunami when they enter lakes or the sea. Landslide-triggered tsunami have been documented in several mountainous areas, including the fjords of Norway (Blikra et al., 2005), Alaska (Coombs et al., 2007), British Columbia (Bornhold et al., 2007; Skvortsov and Bornhold, 2007), Chile, and Greenland (Dahl-Jensen et al., 2004). The steep and high fjord walls in these areas consist of strong rocks with discontinuities on which large masses of rock may suddenly fail. Landslide-triggered tsunami may also originate from large shield volcanoes in the Pacific and Atlantic oceans (Hawaii, Moore et al., 1994; Tenerife, Ward and Day, 2001) and some stratovolcanoes bordering the Pacific Ocean. Waythomas et al. (2009) explore the consequences of several, worst-case hazard scenarios of tsunami triggered by large-scale flank collapses of Alaskan stratovolcanoes.

## 6. Ice-related hazards, floods, and sediment pulses

### 6.1. Characteristics

Many tectonically active mountain belts are characterised by high rates of erosion and sediment yield. Over the past two decades, researchers have shown that catastrophic floods and debris flows resulting from the sudden failure of natural dams are among the most efficient sediment transport processes in mountainous terrain (Clague and Evans, 1994; Cenderelli, 2000; Richardson and Reynolds, 2000; Korup and Tweed, 2007). Indeed, they were the largest floods on Earth during the Quaternary (O'Connor and Costa, 2004). Their volumes and peak discharge follow an inverse power-law trend (Fig. 13), which may be partly linked to the area–frequency distribution of naturally dammed lakes (Fig. 2). Discharge and return periods in partial duration series of palaeofloods also can be modelled by power laws (Malamud and Turcotte, 2006). These statistical relationships should be explored further to gain insights into the recurrence of dam-break events within "normal" fluvial discharge series.

Dam-break floods can severely erode steep reaches along their paths and deposit large amounts of coarse sediment along gently sloping sections of valley floor. The floodwaters mobilise large amounts of sediment as they travel down steep valleys, in some cases producing debris flows (Clague and Evans, 1994). The debris flows have larger discharges and greater destructive impact than the floods from which they form. Relatively little is known about the potential role of these debris flows and others in controlling channel morphology and sediment discharge in alpine headwater channels. Schlunegger et al. (2009) present observations and data from a well-monitored, debris flow-prone torrent in the Rhone River watershed in Switzerland. They highlight the importance of sediment availability for generating frequent events that might elsewhere be regarded as extreme or catastrophic.

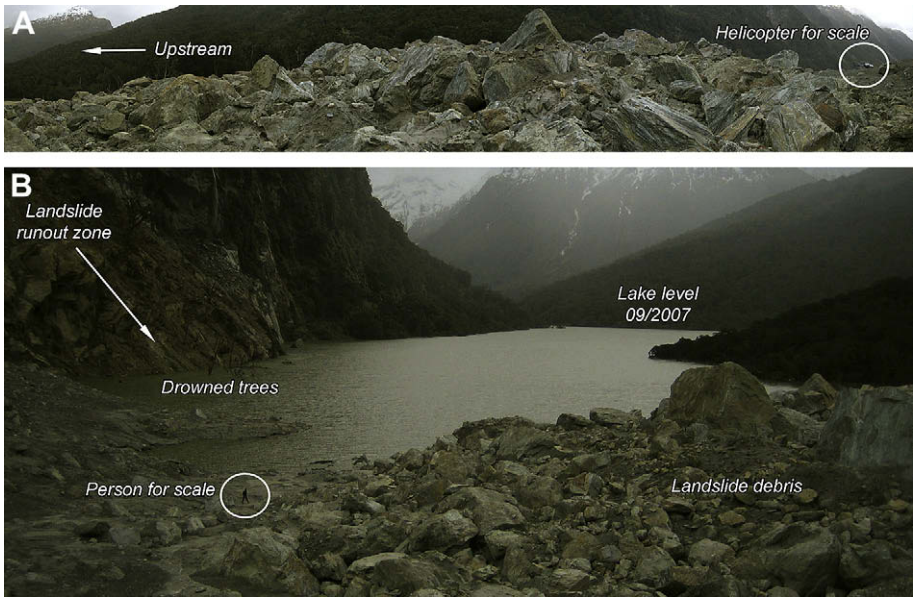


**Fig. 11.** Deposits of catastrophic rock-slope failures in mountainous terrain can be confused with those of glaciers. A. Bouldery debris of the 2007 Young River landslide, Southern Alps, New Zealand. B. The Young River landslide formed a natural dam in a formerly glaciated valley. Distinguishing landslide deposits from moraines is essential for reconstructing glacial history in mountains (Hewitt, 1999).

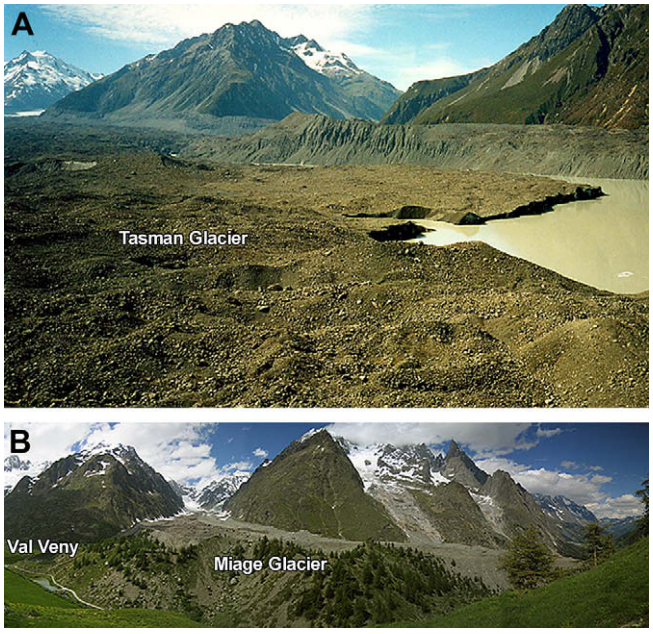


**Fig. 12.** A. The extensive debris cover on Tasman Glacier, New Zealand, is largely due to landslide and rock-fall material deposited on the glacier surface (February 2001). Variations in supraglacial sediment flux may overstate the climatic significance of moraines. B. Debris-covered Miage Glacier, Italian Alps (June 2007). The large, partly vegetated latero-frontal moraine consists mainly of supraglacial debris delivered to the glacier by rock falls and rockslides and carried to the glacier margin.

### 6.2. Palaeofloods in the Quaternary record

Slackwater or backwater deposits can be used to reconstruct the size and frequency of catastrophic prehistoric floods. The extreme end of the spectrum of floods is marked by the gigantic outburst floods from glacial Lake Missoula in the northwest United States. Sequences of slackwater sediments in the Yakima and Walla Walla valleys in Washington state and the Willamette Valley in Oregon, record 40–80 floods (Fig. 14) with peak discharges of up to $10^7$ m$^3$ s$^{-1}$. The floods swept across the Columbia Plateau and down the Columbia River valley between ~17 and 14 ka (Waitt, 1985).

The use of slackwater sediments as flood proxies was pioneered in arid regions because the sediments are more likely to be preserved there (Kochel and Baker, 1988). Yet humid mountain belts, where erosional censoring of such records can be severe (Barnard et al., 2006), also store sediments associated with exceptionally large floods (Montgomery et al., 2004; Srivastava et al., 2008) or very large debris flows (Pratt-Sitaula et al., 2004). Zech et al. (2009) present new $^{10}$Be data on late Holocene landforms in the Annapurna region of the Himalayas, one of the most active orogens on Earth. Ages of boulders on the surfaces of remnant valley fills suggest catastrophic aggradation of the Kali Gandaki River of up to several hundreds of metres in the late Holocene, possibly related to local damming episodes.

### 6.3. Glacier-related hazards

It has been known since the mid-19th century that glaciers have played an important role in shaping mountain landscapes, but understanding the hazards posed by glaciers is a more recent development. The crevassed snouts of glaciers on steep slopes can fail as ice avalanches and, in some cases, transform into large landslides, debris flows, or ice-rock avalanches (Haeberli et al., 2004). Many of the failures are caused by significant changes in glacier mass balance and are triggered by earthquakes or by unusually warm weather, which increases the flow of water at the sole of the glacier.

Recent events have highlighted the potential consequences of 20th century permafrost thaw on the stability of rock slopes in high mountains, particularly where catastrophic rock-slope failures have coincided with times of unusually high air temperatures (Shang

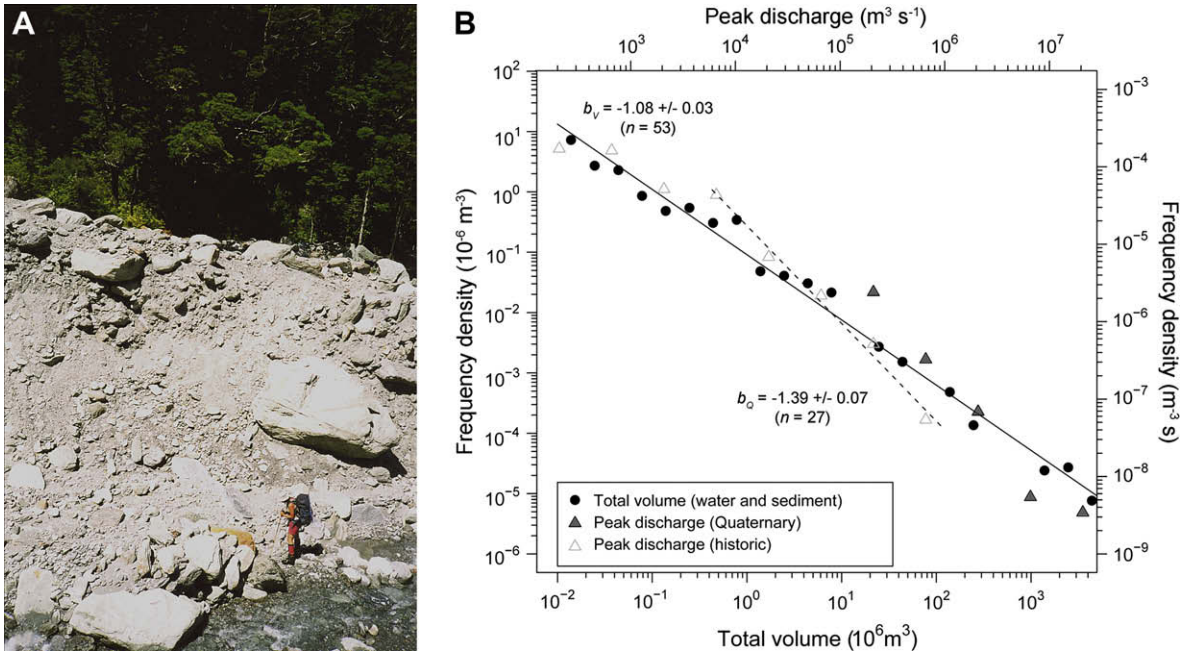


**Fig. 13.** A. Debris flows triggered by sudden drainage of a moraine- or glacier-dammed lake may cause massive aggradation in the valley below the dam. B. Distribution of the total volume and peak discharge of catastrophic outburst flows (floods, hyperconcentrated flows, and debris flows) resulting from failure of historic glacier, moraine, and landslide dams around the world. Total volume and peak discharge show inverse power-law trends (scaling exponents $b_V$ and $b_Q$ are given with $\pm 1\sigma$) over five and two orders of magnitude, respectively. The range of peak discharges overlaps with the lower range of the 27 largest floods of the Quaternary (dark grey triangles; data from O'Connor and Costa, 2004).

**Fig. 14.** Rhythmically bedded, slackwater deposits at Burlingame Canyon, Walla Walla River valley, Washington state. Each couplet in the sequence was deposited a giant outburst flood from glacial Lake Missoula, which was impounded by a lobe of the Cordilleran ice sheet. Approximately 40 couplets are preserved at this site, spanning the period from about 18,000 to 14,000 years ago.

et al., 2003; Gruber et al., 2004). The first reports of these events came from the European Alps, where the density of climate stations is the greatest, but similar temperature-related failures have been reported elsewhere. Huggel (2009) extends this line of research by documenting recent changes in the thermal characteristics of alpine rock slopes, including a range of volcano–ice–rock interactions that have culminated in rock and ice avalanches. Temporal and spatial correlations of rock-mass warming and catastrophic failure are convincing, but leave unanswered questions about the physical processes that have led to sudden detachment of large masses of ice and rock.

## 7. Wildfires

Wildfire is a natural process that renews ecosystems and alters sediment yields in mountains (Shakesby and Doerr, 2006; Jackson and Roering, 2009). The increase in human population in forests and scrublands at the urban-wildland interface in the United States, Australia, Canada, and elsewhere has elevated the risk that wildfires pose to people and property. Well publicized, disastrous wildfires in the western and southwestern United States as well as the devastating 2009 fires in southeast Australia have alerted the public and public officials to this heightened risk.

Less appreciated are the secondary effects of wildfire. Plants and soil are destroyed by severe fire, leaving the mineral soil vulnerable to erosion by impact of raindrops (Robichaud et al., 2000) and runoff. Loss of vegetation and soil due to fire significantly reduces the water storage capacity of soils, thus water runs off more rapidly in burned landscapes than vegetated ones. In addition, organic compounds volatilised by fires and deposited in the soil, inhibit infiltration, thus enhancing runoff (Doerr et al., 2006).

Heavy rainfall after wildfires can generate overland flows that erode mineral soil, creating gullies and rills, and concentrate the sediment in stream channels (Fig. 15; Jackson and Roering, 2009). The severity of erosion in burnt landscapes is complex, as it is influenced by many factors, including: the area and intensity of the burn; the area, hypsometry, and steepness of the catchment; the time, intensity, and duration of rainfall following the wildfire; and antecedent moisture conditions. Sediment concentrated in stream channels after a wildfire can be entrained during severe rainstorms, leading to debris flows (e.g. Cannon, 2001). Although debris flows also occur in unburned forests, wildfires increase the likelihood, number, and size of debris flows during rainstorms.

Much current research addresses the relation between climate and wildfires (e.g., Pierce et al., 2004). Studies based on fire scars on trees and soil charcoal records (Marlon et al., 2006; Gavin et al., 2007; Power, 2008) show a clear link between fire frequency and decadal and centennial drought. However, in the 20th century, this relation, at least in North America, was complicated by large-scale, mechanized, fire-suppression efforts, which had led to a substantial increase in the amount of fuels that feed wildfires and contributed to large and severe burns (Jain et al., 2006).

## 8. Future research directions

Our review shows that extreme events are important components at the tail of systematic and nonlinear magnitude–frequency relationships. These relationships help to estimate the size of events that are most important, in the long term, in shaping landscapes. In the case of landslides, fewer and larger events seem to dominate sediment production rates (Fig. 9). Thus detection and understanding of extremely large landslides may shed new light on long-term erosion rates. A similar dominance of larger events, albeit in terms of total affected area, is evident for many of the processes discussed here (Fig. 2). It seems that the power law is a basis for assessing, to a first order, the size and recurrence of extreme events in recent Earth history. Notably, this relationship seems to hold only for parts of the full frequency–magnitude spectrum for a given process (Malamud et al., 2004). In the future, researchers may want to test more rigorously whether the power law is indeed the best metric of extreme-value distributions (Clauset et al., 2007). Whatever the underlying nonlinear relationship between event frequency and magnitude, the power law helps reveal under-sampled or unidentified events in the Quaternary record and allow estimates to be made of the likelihood of extreme events in the future (Fig. 8).

Importantly, extreme events have caused pronounced, long-lived landscape adjustments, mainly through the sudden release of huge amounts of sediment. The consequences may be more far-reaching and severe than the events themselves; the dynamics and hazard potential of such sediment pulses (Fig. 5) deserve further study. This matter is particularly important in mountainous terrain, because settlements and infrastructure are preferentially located near rivers, which may carry huge amounts of water and sediment following earthquakes, volcanic eruptions, or natural dam failures (Davies and Korup, 2007; Korup and Tweed, 2007). Fluvial response to these disturbances may be very similar, and local and regional events must be carefully distinguished using Quaternary geomorphic and stratigraphic records (Figs. 4 and 5).

Fundamental questions remain about extreme events and their role in Quaternary landscape evolution. For example, 100 years ago a massive explosion caused widespread forest destruction in the Stony Tunguska River area of central Siberia. The cause of this event is still debated – explanations range from the reasonable (an atmospheric explosion of a comet, a meteorite impact, or an explosive decompression of an underground gas reservoir) to the far-fetched (an explosion of an alien nuclear-powered spacecraft) (Steel, 2008). Although large meteorite impacts are rare, they have occurred during the Quaternary. Meteorite (Barringer) Crater in Arizona, for example, is late Pleistocene in age (Phillips et al., 1991), and contested evidence has recently been presented for a meteorite impact 12,900 years cal BP that may have contributed to Younger Dryas cooling and extinction of Pleistocene megafauna (Firestone et al., 2007; Kerr, 2008). The terminal Cretaceous impactor is near

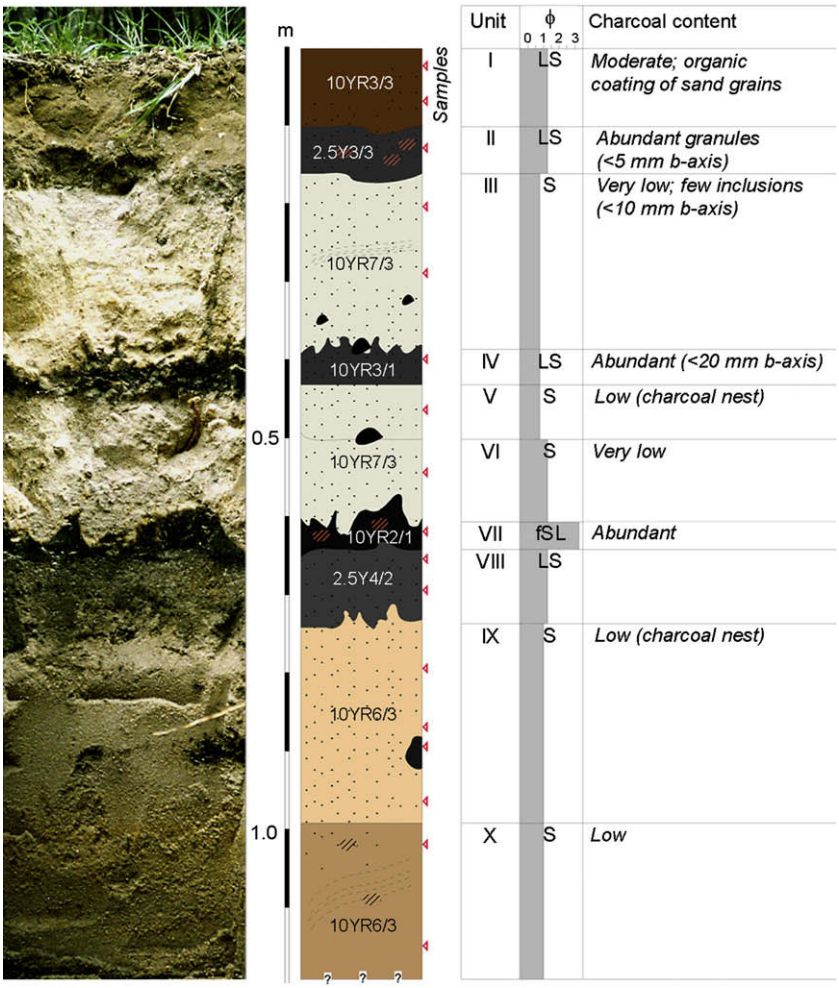


**Fig. 15.** Charcoal-rich layers in fluvial backwater sediments may contain records of sedimentary pulses following wildfires; LS = loamy sand; S = sand; fSL = fine sandy loam (O. Korup, unpubl. data).

the extreme end of the frequency–magnitude scale of bolides that impact Earth (Chapman, 2004). A repeat of such an event today would have a cataclysmic impact on life and the landscape.

## 9. Conclusions

Naturally occurring, but infrequent, extreme events have contributed substantially to shaping mountain landscapes, but what is their importance relative to more frequent, low-magnitude events? This question has been at the core of a still-unresolved debate between uniformitarianists and neo-catastrophists over the efficacy of surface processes in shaping Earth's landscape. Available data and appropriate statistical models now provide the tools to shed light on this question, aided by the identification of extreme events in Quaternary stratigraphic and geomorphic records. New numerical dating techniques provide requisite chronologic control for these events, thus extending limited time series and establishing more robust frequency–magnitude relations that can be used to quantify hazard. Scale-invariant statistical models help in estimating magnitudes and frequencies of hazardous processes such as earthquakes, landslides, floods, and wildfires, and in guiding the search for extreme events in the stratigraphic record. Indeed, natural hazards research and Quaternary sciences have much in common.

## Acknowledgements

We thank Debbie Barrett, Colin Murray-Wallace, and Jim Rose for their encouragement and assistance in assembling the papers that form this Special Issue. We also thank Bodo Bookhagen, Jonathan Carrivick, Paolo d'Odorico, Stuart Dunning, Monique Fort, Alan Gillespie, Stephan Gruber, Aurelia Hubert-Ferrari, Andrew Mackintosh, Matt McGlone, Wilfried Haeberli, Carl Harbitz, Mauri McSaveney, Beth Pratt-Sitaula, Steven Reneau, Alexander Strom, Peter van der Beek, Jeff Warburton, Brian Whalley, Johannes Weidinger, Janet Wilmshurst, Ellen Wohl, and 16 other reviewers who preferred to remain anonymous for helping screen the manuscripts submitted for this Special Issue and improving the quality of those that have been included.

## References

Abele, G., 1974. Bergstürze in den Alpen – ihre Verbreitung, Morphologie und Folgeerscheinungen. Wissenschaftliche Alpenvereinshefte 25.

Allen, A.S.R., Baker, J.A., Carter, L., Wysoczanski, R.J., 2008. Reconstructing the Quaternary evolution of the world's most active silicic volcanic system: insights from an ~1.65 Ma deep ocean tephra record sourced from Taupo Volcanic Zone, New Zealand. Quaternary Science Reviews 27, 2341–2360.

Ambrose, S.H., 1998. Late Pleistocene human population bottlenecks, volcanic winter, and differentiation of modern humans. Journal of Human Evolution 34, 623–651.

Atwater, B.F., Hemphill-Haley, E., 1997. Recurrence Intervals for Great Earthquakes of the Past 3500 years at Northeastern Willapa Bay, Washington. U.S. Geological Survey. Professional Paper 1576.

Barnard, P.L., Owen, L.A., Finkel, R.C., Asahi, K., 2006. Landscape response to deglaciation in a high relief, monsoon-influenced alpine environment, Langtang Himal, Nepal. Quaternary Science Reviews 25, 2162–2176.

Becker, A., Ferry, M., Monecke, K., Schnellmann, M., Giardini, D., 2005. Multiarchive paleoseismic record of late Pleistocene and Holocene strong earthquakes in Switzerland. Tectonophysics 400, 153–177.

Blikra, L.H., Longva, O., Harbitz, C., Løvholt, F., 2005. Quantification of rock-avalanche and tsunami hazard in Storfjorden, western Norway. In: Senneset, K., Flaate, K., Larsen, J.O. (Eds.), Landslides and Avalanches. Proceedings of the 11th International Conference on Landslides. Balkema/Taylor & Francis, London, pp. 57–63.

Bookhagen, B., Thiede, R.C., Strecker, M.R., 2005. Late Quaternary intensified monsoon phases control landscape evolution in the northwest Himalaya. Geology 33, 149–152.

Bornhold, B.D., Harper, J.R., McLaren, D., Thomson, R.E., 2007. Destruction of the First Nations village of Kwalate by a rock avalanche-generated tsunami. Atmosphere-Ocean 45, 123–128.

Brown, E.T., Bendick, R., Bourlès, D.L., Gaur, V., Molnar, P., Raisbeck, G.M., Yiou, F., 2002. Slip rates of the Karakorum fault, Ladakh, India, determined using cosmic ray exposure dating of debris flows and moraines. Journal of Geophysical Research 107 (B9), 2192, doi:10.1029/2000JB000100.

Bull, W.B., 2008. Tectonic Geomorphology of Mountains; A New Approach to Paleoseismology. Wiley–Blackwell, Chichester.

Cannon, S.H., 2001. Debris-flow generation from recently burned watersheds. Environmental and Engineering Geoscience 7, 321–341.

Capra, L., 2006. Abrupt climatic changes as triggering mechanisms of massive volcanic collapses. Journal of Volcanology and Geothermal Research 155, 329–333.

Cashman, K.V., Giordano, G., 2008. Volcanoes and human history. Journal of Volcanology and Geothermal Research 176, 325–329.

Cenderelli, D.A., 2000. Floods from natural and artificial dam failures. In: Wohl, E.E. (Ed.), Catastrophic Flooding. Cambridge University Press, New York, pp. 73–103.

Chapman, C.R., 2004. The hazard of near-Earth asteroid impacts on earth. Earth and Planetary Science Letters 222, 1–15.

Chapron, E., Ariztegui, D., Mulsow, S., Villarosa, G., Pino, M., Outes, V., Juvignie, E., Crivelli, E., 2006. Impact of the 1960 major subduction earthquake in Northern Patagonia (Chile, Argentina). Quaternary International 158, 58–71.

Clague, J.J., 1997. Evidence for large earthquakes at the Cascadia subduction zone. Reviews of Geophysics 35, 439–460.

Clague, J.J., Bobrowsky, P.T., 1994. Tsunami deposits beneath tidal marshes on Vancouver Island, British Columbia. Geological Society of American Bulletin 106, 1293–1303.

Clague, J.J., Evans, S.G., 1994. Formation and failure of natural dams in the Canadian Cordillera. Geological Survey of Canada Bulletin 464.

Clague, J.J., Bobrowsky, P.T., Hutchinson, I., 2000. A review of geological records of large tsunamis at Vancouver Island, British Columbia. Quaternary Science Reviews 19, 849–863.

Clague, J., Yorath, C., Franklin, R., Turner, B., 2006. At Risk; Earthquakes and Tsunamis on the West Coast. Tricouni Press, Vancouver, BC.

Clauset, A., Shalizi, C.R., Newman, M.E.J., 2007. Power-law distributions in empirical data. arXiv:0706.1062v1. [physics.data-an].

Connor, C.B., Sparks, R.S.J., Mason, R.M., Bonadonna, C., Young, S.R., 2003. Exploring links between physical and probabilistic models of volcanic eruptions: the Soufrière Hills Volcano, Montserrat. Geophysical Research Letters 30, 1697–1701.

Coombs, M.L., White, S.M., Scholl, D.W., 2007. Massive edifice failures at Aleutian arc volcanoes. Earth and Planetary Science Letters 256, 403–418.

Cowgill, E., 2007. Impact of riser reconstructions on estimation of secular variation in rates of strike–slip faulting: revisiting the Cherchen River site along the Altyn Tagh Fault, NW China. Earth and Planetary Science Letters 254, 239–255.

Crozier, M.J., Deimel, M.S., Simon, J.S., 1995. Investigation of earthquake triggering for deep-seated landslides, Taranaki, New Zealand. Quaternary International 25, 65–73.

Cruden, D.M., Varnes, D.J., 1996. Landslide types and processes. In: Turner, A.K., Schuster, R.L. (Eds.), Landslides, Investigation and Mitigation. National Research Council, Transportation Research Board, pp. 36–75. Special Report 247.

Dadson, S.J., Hovius, N., Chen, H., Dade, W.B., Lin, J.-C., Hsu, M.-L., Lin, C.-W., Horng, M.J., Chen, T.-C., Milliman, J., Stark, C.P., 2004. Earthquake-triggered increase in sediment delivery from an active mountain belt. Geology 32, 733–736.

Dahl-Jensen, T., Larsen, L.M., Pedersen, S.A.S., Pedersen, J., Jepsen, H.F., Pedersen, G.K., Nielsen, T., Pedersen, A.K., von Platen-Hallermund, F., Weng, W., 2004. Landslide and tsunami 21 November 2004 in Paatuut, West Greenland. Natural Hazards 31, 277–287.

Davies, T.R.H., Korup, O., 2007. Persistent alluvial fanhead trenching resulting from large, infrequent sediment inputs. Earth Surface Processes and Landforms 32, 725–742.

Deline, P., 2009. Interactions between rock avalanches and glaciers in the Mont Blanc massif during the late Holocene. Quaternary Science Reviews 28, 1472.

Doerr, S.H., Shakesby, R.A., Blake, W.H., Chafer, C.J., Humphreys, G.S., Wallbrink, P.J., 2006. Effects of differing wildfire severities on soil wettability and implications for hydrological response. Journal of Hydrology 31, 295–311.

Dortch, J.M., Owen, L.A., Haneberg, W.M., Caffee, M.W., Dietsch, C., Kamp, U., 2009. Nature and timing of large landslides in the Himalaya and Transhimalaya of northern India. Quaternary Science Reviews, 28, 1037–1054.

Dunning, S.A., Mitchell, W.A., Rosser, N.J., Petley, D.N., 2007. The Hattian Bala rock avalanche and associated landslides triggered by the Kashmir earthquake of 8 October 2005. Engineering Geology 93, 130–144.

Dussauge, C., Grasso, J.R., Helmstetter, A., 2003. Statistical analysis of rockfall volume distributions: implications for rockfall dynamics. Journal of Geophysical Research 108 (B6), 2286, doi:10.1029/2001JB000650.

Firestone, R.N., West, A., Kennett, J.P., Becker, L., Bunch, T.E., Revay, Z., Schultz, P.H., Belgya, T., Dickenson, O.J., Erlandson, J.M., Goodyear, A.C., Harris, R.S., Howard, G.A., Kennett, D.J., Kloosterman, J.B., Lechler, P., Montgomery, J., Poreda, R., Darrah, T.H., Que Hee, S.S., Smith, A.R., Stich, A., Topping, W., Wittke, J.H., Wolbach, W.S., 2007. Evidence for an extraterrestrial impact 12,900 years ago that contributed to the megafaunal extinctions and the Younger Dryas cooling. Proceedings of the National Academy of Sciences 104, 16016–16021.

Gavin, D.G., Hallett, D.J., Hu, F.S., Lertzman, K.P., Prichard, S.J., Brown, K.J., Lynch, J.A., Bartlein, P., Peterson, D.L., 2007. Forest fire and climate change in western North America; insights from sediment charcoal records. In: Jackson, S.T. (Ed.), Paleoecology; Using the Past as a Key to the Future. Frontiers in Ecology and the Environment, 5, pp. 499–506.

Girardclos, S., Schmidt, O.T., Sturm, M., Ariztegui, D., Pugin, A., Anselmetti, F.S., 2007. The 1996 AD delta collapse and large turbidite in Lake Brienz. Marine Geology 241, 137–154.

Goff, J.R., McFadgen, B.G., 2002. Seismic driving of nationwide changes in geomorphology and prehistoric settlement – a 15th century New Zealand example. Quaternary Science Reviews 21, 2229–2236.

Gran, K.N., Montgomery, D.R., 2005. Spatial and temporal patterns in fluvial recovery following volcanic eruptions: channel response to basin-wide sediment loading at Mount Pinatubo, Philippines. Geological Society of America Bulletin 117, 195–211.

Gruber, S., Hoelzle, M., Haeberli, W., 2004. Permafrost thaw and destabilization of Alpine rock walls in the hot summer of 2003. Geophysical Research Letters 31, L13504, doi:10.1029/2004GL020051.

Haeberli, W., Huggel, C., Kaab, A., Zgraggen-Oswald, S., Pollkvoj, A., Galushkin, I., Zotikov, I., Osokin, N., 2004. The Kolka-Karmadon rock/ice slide of 20 September 2002; an extraordinary event of historical dimensions in North Ossetia, Russian Caucasus. Journal of Glaciology 50, 533–546.

Hambrey, M.J., Quincey, D.J., Glasser, N.F., Reynolds, J.M., Richardson, S.J., Clemmens, S., 2008. Sedimentological, geomorphological and dynamic context of debris-mantled glaciers, Mount Everest (Sagarmatha) region, Nepal. Quaternary Science Reviews 27, 2361–2389.

Hancox, G.T., Perrin, N.J., 2009. Green Lake landslide and other giant and very large postglacial landslides in Fiordland, New Zealand. Quaternary Science Reviews 28, 1020–1036.

Hewitt, K., 1988. Catastrophic landslide deposits in the Karakoram Himalaya. Science 242, 64–67.

Hewitt, K., 1999. Quaternary moraines vs catastrophic rock avalanches in the Karakoram Himalaya, northern Pakistan. Quaternary Research 51, 220–237.

Hewitt, K., 2009. Catastrophic rock slope failures and late Quaternary developments in the Nanga Parbat–Haramosh Massif, Upper Indus basin, northern Pakistan. Quaternary Science Reviews 28, 1085–1096.

Hewitt, K., Clague, J.J., Orwin, J.F., 2008. Legacies of catastrophic rock slope failures in mountain landscapes. Earth Science Reviews 87, 1–38.

Holm, K., Bovis, M., Jakob, M., 2004. The landslide response of alpine basins to post-Little Ice Age glacial thinning and retreat in southwestern British Columbia. Geomorphology 57, 201–216.

Huggel, C., 2009. Recent extreme slope failures in glacial environments: effects of thermal perturbation. Quaternary Science Reviews 28, 1119–1130.

Hutchinson, I., Guilbault, J.-P., Clague, J.J., Bobrowsky, P.T., 2000. Tsunamis and tectonic deformation at the northern Cascadia margin: a 3000-year record from Deserted Lake, Vancouver Island, British Columbia. The Holocene 10, 429–439.

Jackson, M., Roering, R.R., 2009. Post-fire geomorphic response in steep, forested landscapes: Oregon Coast Range, USA. Quaternary Science Reviews 28, 1131–1146.

Jacoby, G.C., Bunker, D.E., Benson, B.E., 1997. Tree-ring evidence for an A.D. 1700 Cascadia earthquake in Washington and northern Oregon. Geology 25, 999–1002.

Jain, T.B., Graham, R.T., Pilliod, D.S., 2006. The relation between forest structure and soil burn severity. In: Andrews, P.L., Butler, B.W. (Eds.), Fuels Management – How to Measure Success. U.S. Forest Service, Rocky Mountain Research Station, Fort Collins, CO, pp. 615–631.

Jankaew, K., Atwater, B.F., Sawai, Y., Choowong, M., Charoentitirat, T., Martin, M.E., Prendergast, A., 2008. Medieval forewarning of the 2004 Indian Ocean tsunami in Thailand. Nature 455, 1228–1231.

Jibson, R.W., Harp, E.L., Schulz, W., Keefer, D.K., 2006. Large rock avalanches triggered by the M 7.9 Denali Fault, Alaska, earthquake of 3 November 2002. Engineering Geology 83, 144–160.

Jing, L.-Z., Klinger, Y., Sieh, K., Rubin, C., Seitz, G., 2006. Serial ruptures of the San Andreas fault, Carrizo Plain, California, revealed by three-dimensional excavations. Journal of Geophysical Research 111 no. B2.

Karlin, R.E., Holmes, M., Abella, S.E.B., Sylwester, R., 2004. Holocene landslides and a 3500-year record of Pacific Northwest earthquakes from sediments in Lake Washington. Geological Society of America Bulletin 116, 94–108.

Keefer, D.K., 1999. Earthquake-induced landslides and their effects on alluvial fans. Journal of Sedimentary Research 69, 84–104.

Keefer, D.K., Moseley, M.E., 2004. Southern Peru desert shattered by the great 2001 earthquake: implications for paleoseismic and paleo-El Niño–Southern Oscillation records. Proceedings of the National Academy of Sciences 101, 10878–10883.
Kelsey, H.M., Nelson, A.R., Hemphill-Haley, E., Witter, R.C., 2005. Tsunami history of an Oregon coastal lake reveals a 4600 yr record of great earthquakes on the Cascadia subduction zone. Geological Society of America Bulletin 117, 1009–1032.
Kerr, R.A., 2008. Experts find no evidence for a mammoth-killer impact. Science 319, 1331–1332.
Klinger, Y., Sieh, K., Altunel, E., Akoglu, A., Barka, A.A., Dawson, T.E., Gonzalez, T., Meltzner, A.J., Rockwell, T.K., 2003. Paleoseismic evidence of characteristic slip on the western segment of the North Anatolian Fault, Turkey. Bulletin of the Seismological Society of America 93, 2317–2332.
Kochel, R.G., Baker, V.R., 1988. Paleoflood analysis using slackwater deposits. In: Baker, V.R., Kochel, R.G., Patton, P.C. (Eds.), Flood Geomorphology. John Wiley and Sons, New York, pp. 357–376.
Korup, O., 2004. Geomorphic implications of fault zone weakening: slope instability along the Alpine Fault, South Westland to Fiordland. New Zealand Journal of Geology and Geophysics 47, 257–267.
Korup, O., 2006. Effects of large deep-seated landslides on hillslope morphology, western Southern Alps, New Zealand. Journal of Geophysical Research 111, F01018, doi:10.1029/2004JF000242.
Korup, O., Tweed, F., 2007. Ice, moraine, and landslide dams in mountainous terrain. Quaternary Science Reviews 26, 3406–3422.
Korup, O., Clague, J.J., Hermanns, R.L., Hewitt, K., Strom, A.L., Weidinger, J.T., 2007. Giant landslides, topography, and erosion. Earth and Planetary Science Letters 261, 578–589.
Larsen, S.H., Davies, T.R.H., McSaveney, M.J., 2005. A possible coseismic landslide origin of late Holocene moraines of the Southern Alps, New Zealand. New Zealand Journal of Geology and Geophysics 48, 311–314.
Lavé, J., Yule, D., Sapkota, S., Basant, K., Madden, C., Attal, M., Pandey, R., 2005. Evidence for a great medieval earthquake (approximately 1100 A.D.) in the central Himalayas, Nepal. Science 307, 1302–1305.
Lin, G.W., Chen, H., Chen, Y.H., Horng, M.J., 2008. Influence of typhoons and earthquakes on rainfall-induced landslides and suspended sediment yields. Engineering Geology 97, 32–41.
Major, J.J., Pierson, T.C., Dinehart, R.L., Costa, J.E., 2000. Sediment yield following severe volcanic disturbance—a two-decade perspective from Mount St. Helens. Geology 28, 819–822.
Malamud, B.D., Turcotte, D.L., 2006. The applicability of power-law frequency statistics to floods. Journal of Hydrology 322, 168–180.
Malamud, B.D., Turcotte, D.L., Guzzetti, F., Reichenbach, P., 2004. Landslide inventories and their statistical properties. Earth Surface Processes and Landforms 29, 687–711.
Manville, V., Newton, E.H., White, J.D.L., 2005. Fluvial responses to volcanism: resedimentation of the 1800 a Taupo ignimbrite eruption in the Rangitaiki River catchment, North Island, New Zealand. Geomorphology 65, 49–70.
Marlon, J., Bartlein, P.J., Whitock, C., 2006. Changes in fire regimes since the last-glacial maximum; an assessment based on a global synthesis and analysis of charcoal data. The Holocene 16, 1059–1071.
Mason, B.G., Pyle, D.M., Oppenheimer, C., 2004. The size and frequency of the largest explosive eruptions on Earth. Bulletin of Volcanology 66, 735–748.
McGill, S., Sieh, K., 1993. Holocene slip rate of the central Garlock Fault in southeastern Searles Valley, California. Journal of Geophysical Research 98, 14217–14231.
McKillop, R.J., Clague, J.J., 2007. Statistical, remote-based approach for estimating the probability of catastrophic drainage from moraine-dammed lakes in southwestern British Columbia. Global and Planetary Change 56, 153–171.
McSaveney, M.J., 2002. Recent rockfalls and rock avalanches in Mount Cook National Park, New Zealand. In: Evans, S.G., DeGraff, J.V. (Eds.), Catastrophic Landslides; Effects, Occurrence, and Mechanisms. Reviews in Engineering Geology, 15, pp. 35–70.
Meltzner, A.J., Rockwell, T.K., Owen, L.A., 2006. Recent and long-term behavior of the Brawley fault zone, Imperial Valley, California; an escalation in slip rate? Bulletin of the Seismological Society of America 96, 2304–2328.
Messerli, B., Grosjean, M., Hofer, T., Nuñez, L., Pfister, C., 2000. From nature-dominated to human-dominated environmental changes. Quaternary Science Reviews 19, 459–479.
Mitchell, W.A., McSaveney, M.J., Zondervan, A., Kim, K., Dunning, S.A., Taylor, P.J., 2007. The Keylong Serai rock avalanche, NW Indian Himalaya: geomorphology and palaeoseismic implications. Landslides 4, 245–254.
Monecke, K., Finger, W., Klarer, D., Kongko, W., McAdoo, B.G., Moore, A.L., Sudrajat, S.U., 2008. A 1000-year sediment record of tsunami recurrence in northern Sumatra. Nature 455, 1232–1234.
Montgomery, D.R., Hallet, B., Yuping, L., Finnegan, N., Anders, A., Gillespie, A., Greenberg, H.M.D., 2004. Evidence for Holocene megafloods down the Tsangpo River gorge, southeastern Tibet. Quaternary Research 62, 201–207.
Moore, J.G., Bryan, W.B., Ludwig, K.R., 1994. Chaotic deposition by a giant wave, Molokai, Hawaii. Geological Society of America Bulletin 106, 962–967.
Natwidjaja, D.H., Sieh, K., Galetzka, J., Suwargadi, B.W., Cheng, J., Edwards, R.L., Chlieh, M., 2007. Interseismic deformation above the Sunda megathrust recorded in coral microatolls of the Mentwawai Islands, West Sumatra. Journal of Geophysical Research 112 (B2), B02404.
Nur, A., Burgess, D., 2008. Apocalypse: Earthquakes, Archaeology, and the Wrath of God. Princeton Universtiy Press, Princeton, NJ.
O'Connor, J.E., Costa, J.E., 2004. The world's largest floods, past and present: their causes and magnitudes. U.S. Geological Survey Circular 1254, 19.
Oppenheimer, C., 2002. Limited global change due to the largest known Quaternary eruption, Toba ≈ 74 ka? Quaternary Science Reviews 21, 1593–1609.
Owen, L.A., Sharma, M.C., Bigwood, R., 1996. Landscape modification and geomorphological consequences of the 20th October 1991 earthquake and the July–August 1992 monsoon in the Garhwal Himalaya. Zeitschrift für Geomorphologie Supplementband N.F. 103, 359–372.
Owen, L.A., Kamp, U., Khattak, G.A., Harp, E.L., Keefer, D.K., Bauer, M.A., 2008. Landslides triggered by the 8 October Kashmir earthquake. Geomorphology 94, 1–9.
Phillips, F.M., Zreda, M.G., Smith, S.S., Elmore, D., Kubik, P.W., Dorn, R.I., Roddy, D.J., 1991. Age and geomorphic history of Meteor Crater, Arizona, from cosmogenic $^{36}$Cl and $^{14}$C in rock varnish. Geochemica et Cosmochimica Acta 55, 2695–2698.
Pierce, J.L., Meyer, G.A., Jull, A.J.T., 2004. Fire-induced erosion and millennial-scale climate change in northern ponderosa pine forests. Nature 432, 87–90.
Ponomareva, V.V., Melekestsev, I.V., Dirksen, O.V., 2006. Sector collapses and large landslides on late Pleistocene–Holocene volcanoes in Kamchatka, Russia. Journal of Volcanology and Geothermal Research 158, 117–138.
Power, M.J., 2008. Changes in fire regimes since the last glacial maximum; an assessment based on a global synthesis and analysis of charcoal data. Climate Dynamics 30, 887–907.
Prager, C., Zangerl, C., Patzelt, G., Brandner, R., 2008. Age distribution of fossil landslides in the Tyrol (Austria) and its surrounding areas. Natural Hazards and Earth Systems Sciences 8, 377–407.
Pratt-Sitaula, B., Burbank, D.W., Heimsath, A., Ojha, T., 2004. Landscape disequilibrium on 1000–10,000 year scales, Marsyandi River, Nepal, central Himalaya. Geomorphology 58, 223–241.
Pyle, D.M., 2000. Sizes of volcanic eruptions. In: Sigurdsson, H., Houghton, B., Rymer, H., Stix, J., McNutt, S. (Eds.), Encyclopedia of Volcanoes. Academic Press, San Diego, CA, pp. 263–269.
Richardson, S.D., Reynolds, J.M., 2000. An overview of glacial hazards in the Himalayas. Quaternary International 65/66, 31–47.
Robichaud, P.R., Beyers, J.L., Neary, D.G., 2000. Evaluating the Effectiveness of Postfire Rehabilitation Treatments. U.S. Forest Service, Rocky Mountain Research Station, Fort Collins CO.
Schlunegger, F., Badoux, A., McArdell, B.W., Gwerder, C., Schnydrig, D., Rieke-Zapp, D., Molnar, P., 2009. Limits of sediment transfer in an alpine debris-flow catchment, Illgraben, Switzerland. Quaternary Science Reviews 28, 1097–1105.
Schwab, M.J., Werner, P., Dulski, P., McGee, E., Nowaczyk, N.R., Bertrand, S., Leroy, S.A., 2009. Palaeolimnology of Lake Sapanca and identification of historic earthquake signals, Northern Anatolian Fault Zone (Turkey). Quaternary Science Reviews 28, 991–1005.
Shakesby, R.A., Doerr, S.H., 2006. Wildfire as a hydrological and geomorphological agent. Earth-Science Reviews 74, 269–307.
Shang, Y., Yang, Z., Li, L., Liu, D., Liao, Q., Wang, Y., 2003. A super-large landslide in Tibet in 2000: background, occurrence, disaster, and origin. Geomorphology 54, 225–243.
Shennan, I., Bruhn, R., Plafker, G., 2009. Multi-segment earthquakes and tsunami potential of the Aleutian megathrust. Quaternary Science Reviews 28, 7–13.
Shulmeister, J., Davies, T.R., Evans, D.J.A., Hyatt, O.M., Tovar, D.S., 2009. Catastrophic landslides, glacier behaviour and moraine formation a view from an active plate margin. Quaternary Science Reviews 28, 1055–1069.
Skvortsov, A., Bornhold, B., 2007. Numerical simulation of the landslide-generated tsunami in Kitimat Arm, British Columbia, Canada, 27 April 1975. Journal of Geophysical Research 112 (F2), F02028.
Sparks, S., Self, S., Grattan, J., Oppenheimer, C., Pyle, D., Rymer, H., 2005. Super-eruptions. Global effects and future threats. In: Report of a Geological Society of London Working Group. Geological Society of London, pp. 28.
Srivastava, P., Tripathi, J.K., Islam, R., Jaiswal, M.K., 2008. Fashion and phases of late Pleistocene aggradation and incision in the Alaknanda River Valley, western Himalaya, India. Quaternary Research 70, 68–80.
Steel, D., 2008. Tunguska at 100. Nature 453, 1157–1159.
Strasser, M., Anselmetti, F.S., Fäh, D., Giardini, D., Schnellmann, M., 2006. Magnitudes and source areas of large prehistoric northern Alpine earthquakes revealed by slope failures in lakes. Geology 34, 1005–1008.
Strom, A.L., Korup, O., 2006. Extremely large rockslides and rock avalanches in the Tien Shan Mountains, Kyrgyzstan. Landslides 3, 125–136.
Thorardson, T., Larsen, G., 2007. Volcanism in Iceland in historical time: volcano types, eruption styles and eruptive history. Journal of Geodynamics 43, 118–152.
Tovar, S.D., Shulmeister, J., Davies, T.R., 2008. Evidence for a landslide origin of New Zealand's Waiho Loop moraine. Nature Geoscience 1, 524–526.
Turcotte, D.L., Malamud, B.D., Guzzetti, F., Reichenbach, P., 2002. Self-organization, the cascade model, and natural hazards. Proceedings of the National Academy of Sciences 99, 2530–2537.
Waitt Jr., R.B., 1985. Case for periodic, colossal jökulhlaups from Pleistocene glacial Lake Missoula. Geological Society of America Bulletin 96, 1271–1286.
Ward, S.N., Day, S., 2001. Cumbre Vieja Volcano; potential collapse and tsunami at La Palma, Canary Islands. Geophysical Research Letters 28, 3397–3400.
Waythomas, C.F., Watts, P., Shi, F., Kirby, J., 2009. Pacific Basin tsunami hazard-sassociated with mass flows in the Aleutian arc of Alaska. Quaternary Science Reviews 28, 1006–1019.
Wells, A., Goff, J., 2006. Coastal dune ridge systems as chronological markers of paleoseismic activity—a 650 year record from southwest New Zealand. The Holocene 16, 543–550.

Wells, A., Duncan, R.P., Stewart, G.H., 2001. Forest dynamics in Westland, New Zealand: the importance of large, infrequent earthquake-induced disturbance. Journal of Ecology 89, 1006–1018.
Wells, A., Yetton, M.D., Duncan, R.P., Stewart, G.H., 1999. Prehistoric dates of the most recent Alpine fault earthquakes, New Zealand. Geology 27, 995–998.
Wen, B., Wang, S., Wang, E., Zhang, J., 2004. Characteristics of rapid giant landslides in China. Landslides 1, 247–261.
Whitehouse, I.E., Griffiths, G.A., 1983. Frequency and hazard of large rock avalanches in the Central Southern Alps, New Zealand. Geology 11, 331–334.
Witham, C.S., 2005. Volcanic disasters and incidents: a new database. Journal of Volcanology and Geothermal Research 148, 191–233.
Yamaguchi, D.K., Atwater, B.F., Bunker, D.E., Benson, B.E., Reid, M.S., 1997. Tree-ring dating the 1700 Cascadia earthquake. Nature 389, 922.
Yeats, R.S., 2001. Living with Earthquakes in California: a Survivor's Guide. Oregon State University Press, Corvallis, OR.
Zech, R., Zech, M., Kubik, P.W., Kharki, K., Zech, W., 2009. Deglaciation and landscape history around Annapurna, Nepal, based on 10Be surface exposure dating. Quaternary Science Reviews 28, 1106–1118.